JCTC Journal of Chemical Theory and Computation

Theoretical Study of the Photochemical Isomerization of Colchicine

Ivo Cacelli,*,† Maurizio D'Auria,‡ and Vincenzo Villani‡

Dipartimento di Chimica e Chimica Industriale, Università di Pisa, Via Risorgimento 35, 56126 Pisa, Italy, and Dipartimento di Chimica, Università della Basilicata, Via N. Sauro 85, 85100 Potenza, Italy

Received October 17, 2006

Abstract: The photochemical reaction of colchicine to β- and γ-lumicolchicine, through a mechanism involving a disrotatory cyclization, is studied by theoretical methods. The energetics of the reaction, including one or two methanol solvent molecules, are studied at the DFT-B3LYP and multireference perturbation levels of theory using the 6-31G(d) basis set. The results show that, in agreement with experimental results, the first excited state of colchicine at ∼3.6 eV can lead to both β- and γ-lumicolchicine, whose energy is about 15 kcal mol^{-1} above the colchicine energy. Owing to the high steric tension of the condensed four- and five-atom rings arising from cyclization, the two *trans*-lumicolchicines are higher in energy (>60 kcal mol^{-1}), and their formation appears much less probable. A partial inclusion of the solvent effects through the addition of two solvent molecules does not alter the general conclusions based on the free energy in the gas phase. The photochemical reaction path is studied by choosing the distance between the two carbon atoms which form the new σ bond as the leading coordinate of the minimum-energy path of both the ground and the first singlet excited states. The energies are computed by Multi Configurational self-consistent-field calculations on a model molecule, retaining those atoms that presumably play an active role in the reaction. A reasonable mechanism starting from colchicine in the first singlet excited state and leading to γ-lumicolchicine is proposed. On the contrary, a high-energy transition state is found for *trans*-lumicolchicines, whose formation, although not strictly forbidden for energetic reasons, appears to be rather improbable.

Introduction

Colchicine (CC; **1**) is the main alkaloid of the poisonous plant meadow saffron (*Colchicum autumnale* L.),[1] a common plant of European and North African origin that flowers in autumn on a leafless stalk. Besides their use as a poison, the active ingredients of *Colchicum* species belong to the oldest known drugs and have been used for more than 2000 years in the treatment of acute gout. Colchicine (**1**) was first isolated in 1820 by Pelletier and Caventou[2] and is an important bioactive compound used in the treatment of a broad variety of diseases and still remains the sole drug for the therapy of acute gout and familial Mediterranean fever. Moreover, colchicine acts an antimitotic agent by binding to tubulin: it distorts the tubulin/microtubule equilibrium in such a manner that mitosis is arrested in metaphase. Therefore, this compound can be used to selectively damage rapidly proliferating cancer cells.

The irradiation of colchicine leads to the formation of β- and γ-lumicolchicine (β- and γ-LCC; **3** and **4**; Chart 1). Prolonged irradiation times lead to the formation of α-lumicolchicine (**2**) (Chart 1).[2−16]

In a previous study, we reported a pump and probe spectroscopic study on colchicine photoisomerization.[17] After the first excited state was populated by means of irradiation at 360 nm, femtosecond transient spectroscopy showed an

* Corresponding author tel.: +39 050 2219-213; fax: +39 050 2219-260; e-mail: ivo@dcci.unipi.it.

† Università di Pisa.

‡ Università della Basilicata.

10.1021/ct600306t CCC: $37.00
Published on Web 02/02/2007

Chart 1. The Photoisomerization of Colchicine

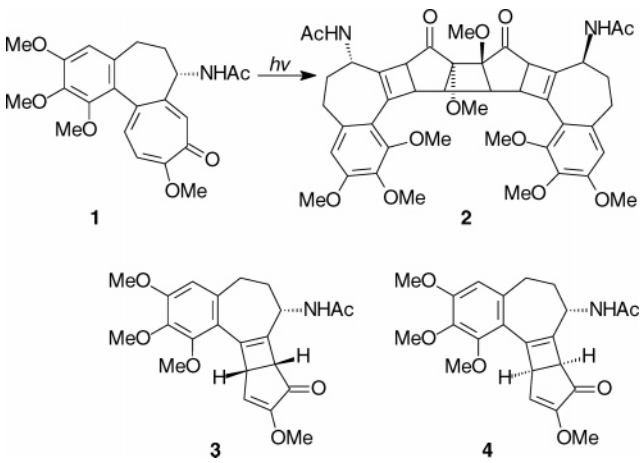

instantaneous strong band with a maximum at 510 nm which disappeared within a few hundred femtoseconds, leaving a broad, structureless band with a maximum around 470 nm. A second band was observed around 410 nm. The analysis in time showed that the 510 nm component appeared instantaneously and decayed following a biexponential law with time constants of 300 ± 100 fs and 40 ps. The kinetics studied by a probe wavelength of 420 nm showed a measurable rise time of 300 ± 150 fs. Transient spectroscopy, as well as theoretical calculations, was in agreement with a mechanism involving a disrotatory cyclization of colchicine in its first excited singlet state to give β- and/or γ-lumicolchicine. The triplet states were considered to play no active role in the process.

In this paper, we report the results of extensive theoretical calculations on colchicine and on the four possible isomers of lumicolchicine. The first study is concerned with the free-energy calculations of the involved molecules; the second step focuses on the decay mechanism from the first excited singlet state of colchicine to the photochemical products.

Method of Calculation

The geometry of the ground state of colchicine and lumicolchicines was optimized without symmetry constraints, both by the Hartree−Fock (HF) method and by density functional theory (DFT) in the B3LYP implementation[18,19] using the 6-31G* basis, which includes a *d* polarization function on the C, N, and O atoms. In order to include some solvent effects, these calculations were repeated including two methanol molecules. They were initially put on the side of the seven-atom ring at a large distance, in order that they be driven by the energy gradient towards the more favorable energetic positions. The solvation energy in methanol was also estimated by the polarizable continuum model[20] (PCM) in which the solvent is treated as a continuum system surrounding the molecule outside a cavity modeled on the molecular shape. HF and DFT calculations were performed with the Gaussian 03 package.[21]

Multireference perturbation theory (MR-PT) calculations were then carried out at the geometries previously optimized at the DFT level, in order to confirm the relative stability of reactants and products. We adopted the CIPSI algorithm[22,23] in which the configurational space is gradually enlarged by

Chart 2. Model System of Colchicine Adopted for the MC-SCF Calculations of the MEP for the S_0 and S_1 States[a]

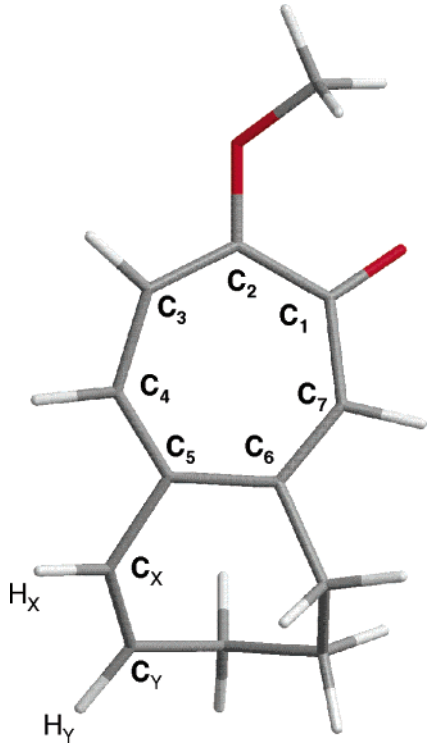

[a] The atom numbering in the reactive seven-atom ring is shown.

exploiting the first-order perturbative correction of the single and double excitations to the ground state. The sequence is repeated until a reasonable compromise between the level of accuracy and the computational effort is reached. In the present work, the final configurational space includes about 6000 detours. The final energy is obtained by second-order diagrammatic perturbation theory in the Möller−Plesset partition scheme, considering the contribution of single and double excitations of this final reference space.

The photochemical reaction under study includes the geometry rearrangement from the first singlet excited state S_1 of colchicine to the ground state S_0 of the four lumicolchicine isomers. Therefore, at least two electronic states have to be considered. In view of the large number of internal coordinates involved in the present reaction, the possibility of building a high-dimensional potential energy surface (PES) for each electronic state is a very complicated task, well beyond the scope of the present paper. A simpler possibility is provided by the minimum energy path (MEP) concept, in which a reaction path is built up by selecting the leading coordinate and optimizing all the remaining internal coordinates at fixed values of the former. An approximate reaction path was thus studied by considering the C_4-C_7 (Chart 2) distance as the leading reaction coordinate, that is, the one which undergoes the most relevant changes along the photochemical reaction. A MEP has to be determined separately both for S_0 and for S_1, in order to account for any possible population of the two states. This requires the nontrivial problem of optimizing the geometry for an excited state without the possibility of exploiting any symmetry restriction.

To save computational time and, at the same time, to avoid possible complications due to mixings of near degenerate excited states localized on the reactive part of the molecule and on the inert six-member ring, the calculation of the reaction path was computed on the model system reported in Chart 2. This was obtained by conserving the reactive molecular region and the aliphatic seven-atom rings adjacent to it. In order to preserve the original steric features, the aromatic ring was substituted by a double CC bond with the length fixed at the typical aromatic value of 1.38 Å. Moreover, the bonded hydrogen atoms H_X and H_Y were constrained to form a HCCH dihedral of 0° ($H_XC_XC_YH_Y$ in Chart 2) in order to mimic the constraints arising from the original aromatic ring. The amide group was substituted by a hydrogen atom. The effectiveness of this stratagem was tested by optimizing the energy of the complete molecule and of the model system. Since the bond lengths of the two calculations do not differ by more than 0.02 Å, the model system was considered adequate for the present study.

The MEPs of both the S_0 and S_1 states were computed by Multi Configurational self-consistent-field (MC-SCF) calculations in the restricted active space formulation, including the five higher occupied molecular orbitals (MOs) and the five lowest empty MOs in the active space. All the single and double excitations in the active space were included in the configurational space. The active space (10 MOs and 10 electrons) involves all the π and π^* orbitals in CC, including even the C_X-C_Y π bond (Chart 2), which is not involved in conjugation. In LCC, there are only four π orbitals, and the active space includes the lone-pair orbital on the methoxy group with the exclusion of the newly formed C_4-C_7 bond. Therefore, the active space appears to be slightly unbalanced for the reagent and the products. On the other hand, a better description of the formation of the C_4-C_7 bond would require the inclusion of all the valence orbitals, but this is not possible for computational reasons. The two states were computed using state-averaged two-states calculations with equal weights, in order to avoid root flipping problems. Geometry optimization was thus performed at several C_4-C_7 distances considering both S_0 and S_1 as the reference state. The MOLPRO program[24] was used for MC-SCF calculations.

Results and Discussion

Energy and Geometrical Structure of the Reagent and Products. Chart 3 displays a schematic picture of the four isomers β, γ, trans-1, and trans-2 of lumicolchicine. The β and γ isomers differ from each other in the position of the amide group with respect to the five-membered ring containing the carbonyl and methoxy groups. In the β isomer, the amide and carbonyl groups are on the same side with respect to the $C_4-C_5-C_6-C_7$ plane and may form an intramolecular hydrogen bond. Conversely, in the γ isomer, these groups are much more distant and cannot interact appreciably. In both the trans conformers, the two condensed rings lie roughly in the same plane and no direct interaction with the amide group can occur. Their geometrical difference can be again referred to the amide group: in the trans-1 conformer, the C_7-H bond is on the same side as the amide group, whereas in the trans-2 conformer, the C_7-H bond is on the opposite side.

Chart 3. The Reactive Molecular Energy Region of the Four Isomers of Lumicolchicine

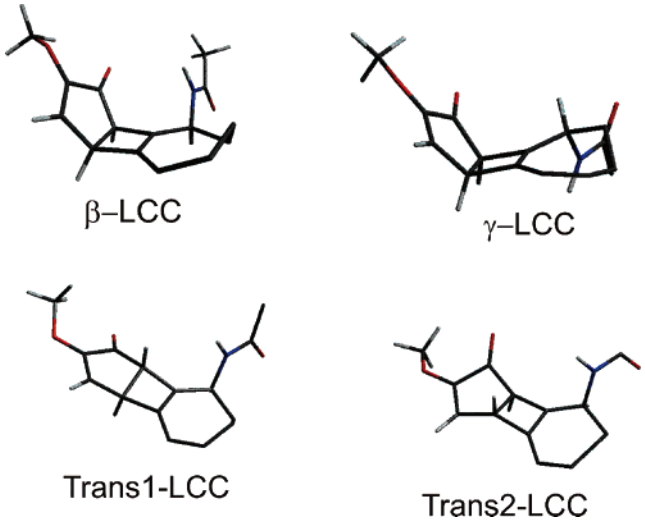

The relative energies of CC and the four isomers of LCC at the optimized geometries obtained by several methods are reported in Table 1. The table includes also the low-level HF/6-31G results for comparison and the zero-point energy (ZPE) correction as well as an estimate of the solvation energy with the explicit inclusion of two methanol molecules and with the PCM method. Some structural parameters referred to the B3LYP-optimized geometry are reported in Table 2.

The HF and B3LYP calculations give similar results, and also the correlated MR-PT treatment shows that the trans forms of LCC are much higher in energy than the β and γ conformers. This is due to the steric tension of the reactive seven-atom ring in both the *trans*-LCCs where the trans position of the hydrogen atoms bonded to the C_4 and C_7 atoms generates a large distortion from planarity in both of the two condensed rings [see the root-mean-square (RMS) column of Table 2]. The small difference in stability between the β and γ conformers can probably be ascribed to an intramolecular hydrogen bond between the carbonyl group and the H atom of the amide group, which occurs for β-LCC. This is clearly indicated by the O−N distance reported in the last column of Table 2: 2.1 Å for β-LCC versus 4.5 Å for γ-LCC.

Since we are interested in the photochemical reaction of CC in solution, this apparent stability of β-LCC versus γ-LCC obtained in gas-phase calculations (about 4 kcal mol^{-1}) could have a weak meaning. For this reason, we have performed a further calculation in which two methanol solvent molecules have been added to the systems under scrutiny. As explained in the previous section, the geometry optimization starts with the two solvent molecules placed at a large distance from the reactive molecular region, in order not to show bias between the different possibilities of forming solute−solvent hydrogen bonds. In the optimized geometry of β-LCC, one methanol molecule interposes between the carbonyl group and the amidic hydrogen, destroying the intramolecular hydrogen bond observed in the isolated

Table 1. Relative Energy of Colchicine (CC) and Lumicolchicines (LCC) at Their Equilibrium Geometries (kcal mol^{-1})[a]

method	basis set	CC	β-LCC	γ-LCC	*trans*-1-LCC	*trans*-2-LCC
HF/6-31G	6-31G	0.00[b]	14.03	18.38	74.47	71.06
B3LYP	6-31G*	0.00[c]	12.54	16.83	62.09	61.73
MR-PT[d]	6-31G*	0.00[e]	16.39	17.13	61.94	61.88
B3LYP + 2S[f]	6-31G*	0.00	10.73	11.15	64.92	64.80
B3LYP+PCM	6-31G*	0.00	16.53	16.89	61.78	62.53
ZPE (B3LYP)	6-31G*	277.18	276.99	276.74	275.30	276.24
B3LYP+ZPE	6-31G*	0.00	12.35	16.39	61.21	60.79

[a] Apart from HF, all other results are obtained with the 6-31G* basis set. [b] Absolute energy HF/6-31G is −1350.628764 H at HF optimized geometry. [c] Absolute energy B3LYP/6-31G* is −1359.417458 H. [d] Calculations at the geometry optimized at the B3LYP level. [e] Absolute energy −1340.416360 H. [f] Including two methanol molecules.

Table 2. Value of Some Relevant Internal Coordinates at Equilibrium Geometry (Å or Degrees) by B3LYP/6-31G* Calculations

	C_4-C_7	C_4-C_5	C_5-C_6	C_6-C_7	θ (RMS)[a]	C_1-C_2	O−HN
CC	3.06	1.38	1.44	1.37	3.3 (0.002, 0.028)	1.48	4.70
β-LCC	1.56	1.54	1.36	1.53	62.0 (0.003,0.009)	1.49	2.13
γ-LCC	1.56	1.55	1.36	1.52	61.5 (0.000,0.001)	1.49	4.51
trans-1-LCC	1.55	1.55	1.37	1.54	13.7 (0.047,0.202)	1.55	4.80
trans-2-LCC	1.55	1.55	1.37	1.54	14.2 (0.041,0.208)	1.55	3.86

[a] Angle between the two least-squares planes given by the $C_4-C_5-C_5-C_7$ and $C_1-C_2-C_3-C_4-C_7$ atoms. The root-mean-square (RMS) value (in Å) of the two least-squares planes is reported in parentheses.

β-LCC molecule. Apart from this particular behavior observed only for the β-LCC conformer, in all the other cases, the methanol molecules form hydrogen bonds with the ether, carbonyl, or amide groups of both CC and LCCs. The relative energies from these new calculations show, however, that the fraction of solvation energy accounted for two solvent molecules does not upset the relative stability of the conformers in the gas-phase calculations. The slightly smaller solvation energy of β-LCC with respect to γ-LCC can probably be ascribed to the destruction of the already discussed intramolecular hydrogen bond between the carbonyl and the amide groups. The geometries optimized by accounting for the solvent effects through the PCM method show no trace of an intramolecular hydrogen bond, and the PCM solvation energy is similar for CC and for the four LCC conformers. All of these results allow us to assess that the solvent effect does not affect significantly the relative stability of the four LCC isomers.

Even the inclusion of the ZPE in the total molecular energy has small effects on the energetic gaps between the several LCCs (last row of Table 1). The free energy obtained by the inclusion of the entropic contribution of the vibrational degrees of freedom changes the energy differences by no more than 0.5 kcal mol^{-1}. Therefore, the computed relative energies of the LCC isomers appear to be rather stable both versus solvation and versus vibrational contributions.

The relative stabilities of CC and the LCCs are now considered in the light of the photochemical reaction in which colchicine undergoes a transition to the first singlet excited state and decays to γ-LCC and β-LCC. Since the absorption band of CC is centered at 3.65 eV (84 kcal mol^{-1}), from the energy criterion, all four of the LCCs could in principle be obtained, even if the energy of the *trans*-LCCs lie only about 20 kcal mol^{-1} below the maximum energy allowed for the products. However, the higher stability of both the cis conformers with respect to the *trans*-LCCs makes the former much more probable, and the present theoretical data are in full agreement with experimental results. Moreover, the high energy of all the LCCs with respect to the thermal energy precludes the possibility of thermal interconversion from CC to LCC, in agreement with observations.

The present data confirm the theoretical investigations reported in previous papers.[17,25] In the hypothesis that the first excited state of CC at 3.65 eV corresponds essentially to a singlet highest occupied molecular orbital → lowest unoccupied molecular orbital (HOMO → LUMO) transition, the spatial distribution of the LUMO of CC was carefully analyzed,[4] and it was verified that a disrotatory process could lead to a C_4-C_7 bonding, rather than antibonding, σ orbital. This feature was considered consistent both with the presence of a low-energy transition state and with the formation of *cis*-LCC isomers. The present data confirm the previous analysis and add the valuable information that the trans conformers are less stable.

From the C−C bond lengths reported in Table 2, it is apparent that the C_4-C_7 distance does not change along the LCC series. Even the other C−C bond lengths in the two condensed rings show the typical values of single and double C−C bonds for all LCC isomers: for instance, the C_4-C_5 and C_6-C_7 bond lengths are consistent with a double and, respectively, single C−C bond. From the C−C bond lengths of colchicine, it seems that the seven-atom ring has a reduced π aromaticity, since the C_4-C_5 and C_6-C_7 bonds show the typical double-bond length (1.34 Å). On the contrary, the C_5-C_6 bond length in CC is shorter than the typical C−C single bond distance (>1.5 Å). The latter feature may probably be ascribed to the fact that the C_5-C_6 bond is included in the nonplanar seven-atom ring (lower part of Chart 2) which, due the presence of both sp^2 and sp^3 carbon atoms, is affected by some degree of steric tension.

Whereas in the *cis*-LCCs (both β and γ) the two condensed rings are nearly planar and form an angle of about 60° (sixth

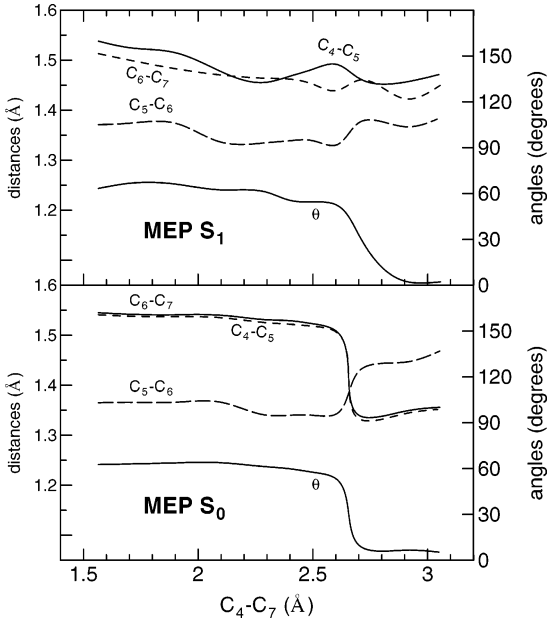

Figure 1. Values of some internal coordinates (Å or deg) versus the C_4-C_7 distance along the MEP of the S_0 and S_1 states connecting the γ-lumicolchicine with the colchicine. All the remaining internal coordinates are optimized for the model system of Chart 2 at the MC-SCF/6-31G* level of theory. θ is the angle between the two least-squares planes given by the $C_4-C_5-C_5-C_7$ and $C_1-C_2-C_3-C_4-C_7$ atoms (Chart 2).

column of Table 2), in the trans conformers, the same rings are nearly coplanar but their atoms strongly deviate from coplanarity, as indicated by the high RMS values of the least-squares planes. This supports a high steric tension in both rings, which is the basic reason for the instability of the trans conformers. Finally, the distance between the carbonyl oxygen and the amidic hydrogen, reported in the last column of Table 2, indicates an intramolecular hydrogen bond in β-LCC, as above-mentioned.

Geometrical Rearrangements along the S_0 and S_1 MEPs. In Figure 1, we report the values of some internal coordinates which undergo large changes along the transformation from CC to LCC, versus the leading internal coordinate C_4-C_7 distance. The reported values refer to geometries separately optimized for S_0 and S_1 at the MC-SCF level for the model system of Chart 2. In order to avoid the complications arising from the intramolecular hydrogen bond involving the amide group in β-LCC, we have considered the MEP connecting CC to the γ-LCC isomer. The corresponding energy curves of the MEPs are reported in Figure 2 [$E_0(0)$ and $E_1(1)$ respectively for S_0 and S_1] and will be discussed later on.

Since the S_1 state roughly corresponds to a $\pi \rightarrow \pi^*$ (HOMO $\rightarrow$ LUMO) excitation[4] localized on the reactive region both for CC and for LCCs, a general decrease of the bond orders and an increase of the bond lengths are expected in the seven-atom rings, on going from S_0 to S_1. From Figure 1, it is apparent that this effect is more pronounced in colchicine, indicating that the electronic excitation causes a destabilization on the seven-atom ring. The main geometrical changes are concerned with the bond length of the $C_4-C_5-C_6-C_7$ sequence, which roughly corresponds to $C_4=C_5-C_6=C_7$ and $C_4-C_5=C_6-C_7$ for S_0 and S_1, respectively. This is a very interesting feature since the bond lengths undergo moderate changes along the S_1 MEP and are similar to those of γ-lumicolchicine. Therefore, the geometrical relaxation of S_1 in the reagent (and presumably in the early stage of the reaction) gives rise to a structure consistent with the observed photochemical reaction.

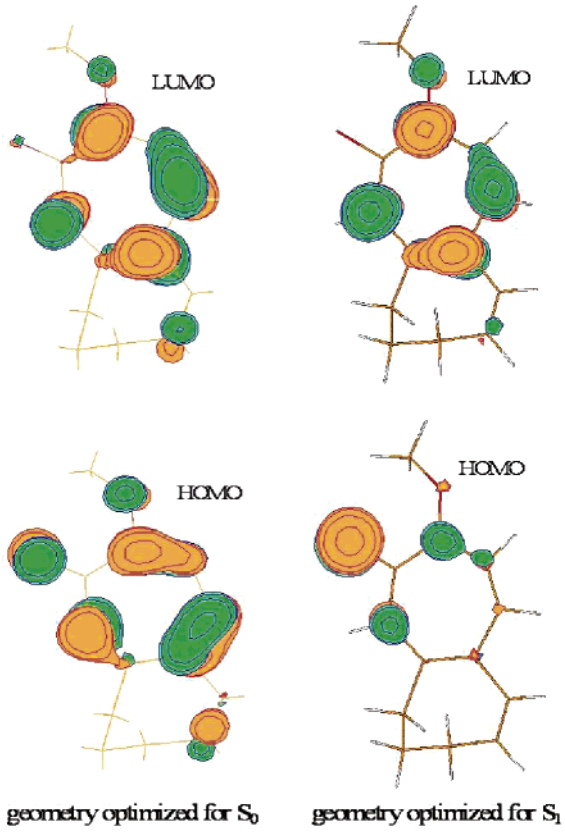

Figure 2. Map of the HOMO and LUMO of the colchicine model system of Chart 2. Left: the geometry is that optimized for the ground state. Right: relaxed geometry for the S_1 state. The MOs are the natural orbitals of MC-SCF calculations.

The profile of the MEP curves of Figure 1 indicates that the most relevant geometrical changes occur in a small range of C_4-C_7 distances, namely, in the 2.6−2.7 Å range, where the seven-membered ring bends towards an angle of about 60°. This geometrical change is more evident for S_0 where the θ change is accompanied by sharp changes in the bond lengths, corresponding to a shift from a single to double bond or vice versa. For S_1, the change of the interplane angle θ is less rapid, and it is accompanied by smaller changes of the C−C bond lengths with no net increment/decrement of one unit of bond order. As discussed above, the flatness of the curves in the S_1 MEP probably derives from the fact that the S_1 geometrical relaxation in colchicine (without changing the C_4-C_7 distance) gives bond lengths similar to those observed in the four-atom ring of the products.

Analysis of the Molecular Orbitals. A partial rationale of this behavior can be found by analyzing the HOMO and LUMO of the S_0 and S_1 MEPs at a value of the C_4-C_7 distance of 3.05 Å, corresponding to CC. The MOs are displayed in Figure 2. The HOMO and LUMO at the S_0 MEP are typical of conjugate systems: both are π orbitals, and

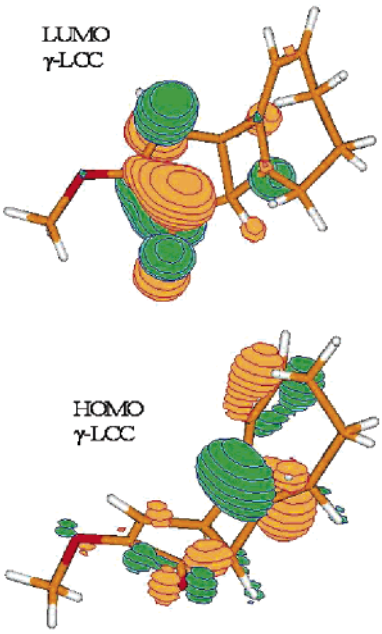

Figure 3. Map of the HOMO and LUMO of the γ-lumicolchicine model system of Chart 2. The MOs are the natural orbitals of MC-SCF calculations.

the LUMO has one more node than the HOMO. The HOMO seems to give a noticeable contribution to the double bonds of the seven-atom ring with some contribution on the carbonylic oxygen. In the relaxed geometry (i.e., optimized for S_1 at $C_4-C_7 = 3.05$ Å), the LUMO is similar to the previous one but the HOMO is almost completely localized on the carbonylic oxygen (nonbonding), and it is very different from the HOMO at the S_0 MEP. This finding is in accord with the data of Figure 1 for CC, where on going from the S_0 MEP to the S_1 MEP a remarkable increase of the C_4-C_5 and C_6-C_7 distances was observed, together with a decrease of the C_5-C_6 bond length. Indeed, since the HOMO at the S_0 MEP is bonding for the C_4-C_5 and C_6-C_7 bonds and antibonding for the C_5-C_6 bond, its migration towards the carbonyl group reinforces the first two bonds and weakens the latter.

The two LUMOs of Figure 2 remain similar along their own MEPs, and both move towards the C_1-C_2 bond (see Figure 3). The HOMO of the S_0 MEP localizes in the C_4-C_7 region along the path, gives a relevant contribution to the formation of the new σ bond, and finally becomes a π bonding orbital on the C_5-C_6 bond in the four-atom ring of LCC (see Figure 3). The HOMO of the S_1 MEP (also called HSOMO) is localized on the carbonylic oxygen in CC, shifts partially to the C_7 atom, and becomes similar to the HOMO of the S_0 MEP in γ-LCC. Thus, it appears that for γ-lumicolchicine the HOMO and the LUMO are localized on different rings and we may expect a weak transition to the first excited state.

Energetics of the Reaction Path. The MC-SCF energies of the ground state S_0 and of the first singlet excited state S_1 along the MEP connecting colchicine and γ-lumicolchicine are displayed in Figure 4. The four curves (the *trans*-1-LCC curve will be considered later on) refer to the energy of the S_0 and S_1 states computed along the S_0 MEP and S_1 MEP

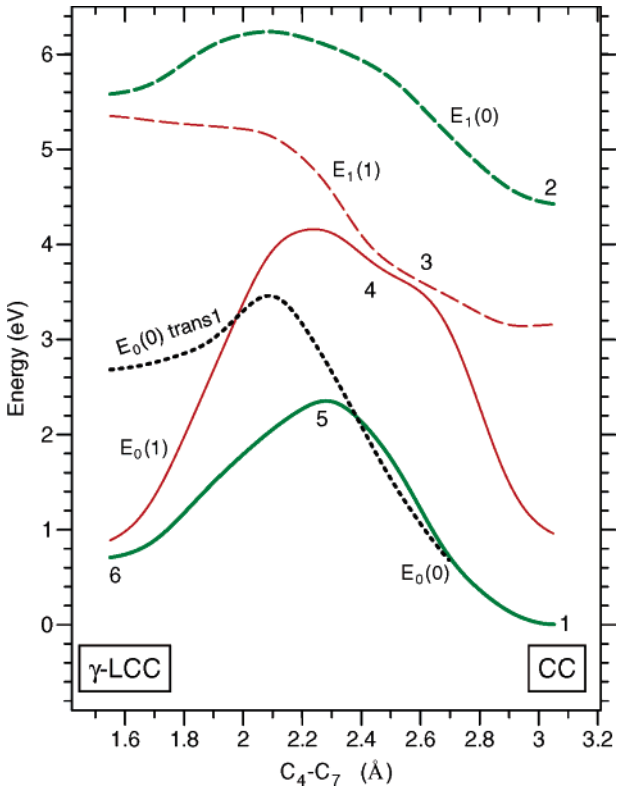

Figure 4. Energy of the S_0 (E_0, full lines) and of the S_1 (E_1, dashed lines) states along their own MEP leading to γ-lumicolchicine. The 0 in parentheses indicates the S_0-MEP (green heavy lines); the 1 indicates the S_1-MEP (red light lines). The MEP of S_0 leading to trans-1-lumicolchicine is also reported. The numbers 1−6 refer to the discussion in the text.

(label in parentheses). For instance, the curve labeled $E_1(0)$ in Figure 4 refers to the S_1 energy computed at the geometries optimized for S_0. Thus, the $E_1(0) - E_0(0)$ energy difference represents the vertical excitation energy at the geometry optimized for S_0 for a given C_4-C_7 distance. $E_1(0) - E_1(1)$ is the relaxation energy of the excited state due to the change of the internal coordinates other than the fixed C_4-C_7 distance. The CI expansion coefficients of the MC-SCF states indicate that at all geometries S_0 and S_1 always have a closed shell and a single excited configuration, respectively.

The $E_0(0)$ energy curve represents the minimum energy path of a thermal photoisomerization. The barrier for this process is about 2.4 eV (~52 kcal mol^{-1}), which prevents this reaction from spontaneously proceeding, in agreement with the experimental evidence.

A clear difference between the two shown MEPs is that the $S_0 \rightarrow S_1$ excitation energy calculated along the S_0 MEP $[E_1(0) - E_0(0)]$ is always higher than 4 eV, whereas the same quantity calculated along the S_1 MEP $[E_1(1) - E_0(1)]$ is high in proximity to the reagents and products but is small in the 2.2−2.8 Å range. In particular, S_0 and S_1 are near degenerate along the S_1 MEP, in the 2.4−2.6 Å range, and this could enhance the probability of surface hopping. It is noteworthy that, in this range, the inter-ring angle is close to 60°; that is, the seven-atom ring is bent (see Figure 1). Therefore, on going from CC to γ-LCC, the bending of the seven-atom ring atom occurs when the C_4-C_7 distance is well higher than the typical C−C single bond length.

On the basis of the data reported in Figure 4, we may attempt to sketch a possible reaction mechanism with the help of the numbers 1−6, as reported in the figure. Colchicine (point 1) absorbs one photon, and the S_1 state at the same geometry (point 2) is populated through a sudden vertical photoexcitation. The S_1 state undergoes a geometry relaxation, and the representative point moves from point 2 to point 3 towards smaller C_4-C_7 values and smaller energies. From Figure 1, it is apparent that in the 2 → 3 step the θ angle increases and the bond distances involving the C_4, C_5, C_6, and C_7 atoms move towards the values they take in LCC. Notice that in this step the energy of S_0 increases by more than 2 eV [$E_0(1)$ curve] and approaches the $E_1(1)$ curve. The next step towards point 4 involves a possible nonadiabatic transition to the S_0 PES. The 4 → 5 step is concerned with the geometrical relaxation of S_0, and finally, the system can flow on the PES of S_0 towards point 6, co-incident with the γ-LCC product.

It is worth noticing that all of the hypothesized steps proceed with a decrease of the potential energy and that no barrier is observed for the proposed mechanism. The rate-determining step is likely to be the nonadiabatic transition from S_1 to S_0 around 2.5 Å.

The dotted curve reported in Figure 4 is the energy of the ground state along the reaction path of S_0 connecting colchicine with *trans*-1-lumicolchicine, computed as previously done for the γ conformer. For C_4-C_7 values greater than 2.6 Å, the reaction paths for *trans*- and *cis*-LCCs are identical, since the seven-atom ring is nearly planar. For lower values of C_4-C_7, the *trans*-1-LCC curve shows an energy maximum of about 3.4 eV at 2.1 Å. Since both the energies of the final state and of the transition state are lower than the energy of point 2, the formation of a low quantity of *trans*-1-LCC cannot be completely excluded by the present data.

Finally, a pictorial view of the electronic rearrangement along the S_0 MEP is reported in Figure 5. The contour lines refer to the projection of the electron density of S_0 onto the plane containing both the C_4 and C_7 atoms and bisecting the angle formed by the planes of the four- and five-atom rings. The disrotatory cyclization process and the C_4-C_7 σ-bond formation is apparent for C_4-C_7 distances shorter than 2.60 Å, where the two condensed rings bend towards an interplane angle of about 60°. The geometrical changes of the hydrogen atoms bonded to C_4 and C_7 can be estimated by observing the deformation of the density from the circular form. These hydrogen atoms are seen to deviate from a nearly collinear $H-C_4-C_7-H$ sequence in colchicine to C−C−H angles close to the typical tetrahedral value in γ-lumicolchicine. The corresponding contour map of S_1 is very similar with a small increase of density for C_4-C_7 in the 2.40−2.40 Å range and does not allow quantitative conclusions about the different electronic structures of the two states.

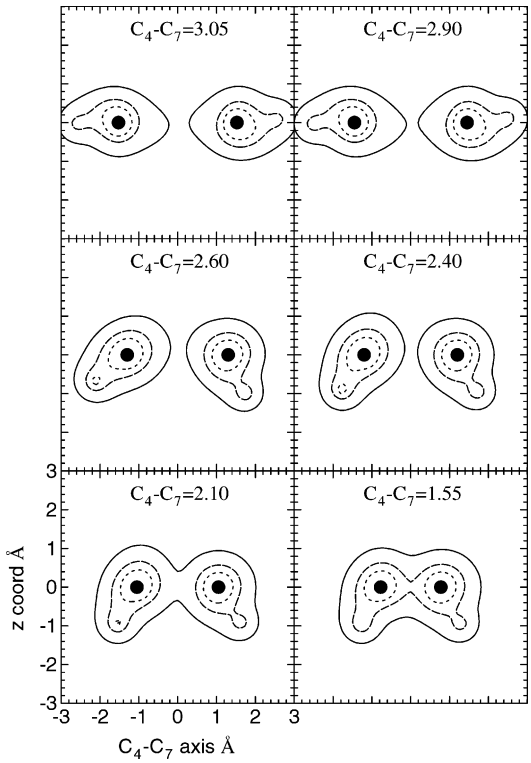

Figure 5. Contour map of S_0 electron density along the S_0-MEP. The density is projected onto the plane containing both the C_4 and C_7 atoms and bisecting the angle formed by the $C_4-C_5-C_5-C_7$ and $C_1-C_2-C_3-C_4-C_7$ least square. The abscissa axis is the line connecting C_4 and C_7; the ordinate (*z* coordinate) is the orthogonal line on the plane. The C_4 and C_7 atoms are indicated as full circles. The contour lines correspond to density values of 0.05, 0.15, and 0.25.

Conclusions and Final Remarks

From the computed energies of colchicine and the four possible isomers of lumicolchicine, it is argued that the β and γ conformers are strongly favored as possible products of the intramolecular photocyclization reaction. The energy profiles of the ground and the first singlet excited states allow tracing a possible reaction path, using the distance of the two carbon atoms forming the new σ bond as the leading coordinate. The geometrical rearrangement of the excited state is consistent with the geometry of the products, and all of the results are consistent with the experimentally observed formation of β and γ conformers.

In the present paper, the theoretical study has been driven by a hypothesized reaction path in accordance with experimental evidence. However, this paper pretends neither to explain completely the reaction under study nor to exclude other possible paths leading to different products. For instance, for similar systems like tropolone derivatives, it was found that an analogous photochemical reaction leads to the formation of a new σ bond between the C_1 and C_5 atoms.[26,27] The study of the MEP provides useful information but does not account for the dependence on the initial dynamic conditions of the reactant nor for possible deviations of the reactive trajectories from the MEPs. However, it has been stated that reactions in solution have more of a chance to proceed along MEPs since the excess energy is more easily dissipated through the solvent interaction. The experimentally observed rapid decay of S_1 with time constants of 300 fs could indicate an instantaneous geometrical rearrangement, in agreement with the present results which show that the relaxation energy of S_1 is about 1 eV. The second slow decay pattern with a time constant of 40 ps is consistent with the

possibility that the isomerization reaction may only occur through a well-defined path, which, presumably, involves small deviations from the MEP.

The hypothesized mechanism does not include possible intersystem crossing with triplet states. In order to check for this possibility, which however does not seem in agreement with experimental evidence, the energy curve of the lowest triplet state T_1 and the spin−orbit coupling between S_1 and T_1 were computed along the MEP of S_1 for C_4-C_7 values greater than 2.4 Å. It was found that T_1 always has a lower energy than S_1 with no crossing and that the spin−orbit coupling between these two states does not exceed 0.5 cm^{-1}. From these results, it appears that the role of T_1 in the studied photochemical isomerization is irrelevant. This is in accord with an experimental study in which no quenching effect was observed in the reactivity, in the presence of several triplet acceptors.[28] The opposite is expected for the same reaction in tiocolchicine, where no photoisomerization was observed and S_1 dissipates its excess energy in a different way.[25] This study will be the object of a future work.

Acknowledgment. I.C. acknowledges the MURST (Ministero della Ricerca Scientfica e Tecnologica: cofinanziamento 2004) for financial support. V.V. acknowledges CASPUR (University La Sapienza, Rome, Italy) for the use of computational resources.

References

(1) Capraro, H. G.; Brossi, A. In *The Alkaloids*; Brossi, A., Ed.; Academic Press: New York, 1984; Vol. 23, pp 1−70.

(2) Pelletier, P. J.; Caventou, J. B. *Ann. Chim. Phys*. **1820**, *14*, 69.

(3) Canonica, L.; Danieli, B.; Manitto, P.; Russo, G. *Tetrahedron Lett.* **1969**, 607−608.

(4) Chapman, O. L.; Smith, H. G.; King, R. W. *J. Am. Chem. Soc*. **1963**, *85*, 803−812.

(5) Forbes, E. J. *J. Chem. Soc*. **1955**, *9*, 3864−3870.

(6) Gardner, P. D.; Brandon, R. L.; Haynes, G. R. *J. Am. Chem. Soc*. **1957**, *79*, 6334−6337.

(7) Gasic, O.; Popovic, M. *Herba Hung.* **1981**, *41*, 51−54.

(8) Husek, A.; Sutlupinar, N.; Sedmera, P.; Voegelein, F.; Valka, I.; Simanek, V. *Phytochemistry* **1990**, *29*, 3058−3060.

(9) Malichova, V.; Potesilova, H.; Preininger, V.; Santavy, F. *Planta Med.* **1979**, *36*, 119−127.

(10) Merchant, J. R.; Joshi, V. *Indian J. Chem., Sect. B: Org. Chem. Incl. Med. Chem.* **1976**, *14*, 908−911.

(11) Pijsewska, L.; Kaul, J. L.; Joshi, R. K.; Santavy, F. *Collect. Czech. Chem. Commun.* **1967**, *32*, 158−170.

(12) Potesilova, H.; Acaraz, C.; Santavy, F. *Collect. Czech. Chem. Commun.* **1969**, *34*, 2128−2133.

(13) Potesilova, H.; Wiedermannova, J.; Santavy, F. *Collect. Czech. Chem. Commun.* **1969**, *34*, 3642−3645.

(14) Santavy, F. S. P.; Snatzke, G.; Reichstein, J. *Helv. Chim. Acta* **1971**, *54*, 1084−1095.

(15) Sutlupinar, N.; Husek, A.; Potesilova, H.; Dvorackova, S.; Hanus, V.; Sedmera, P.; Simanek, V. *Planta Med.* **1988**, *54*, 243−245.

(16) Takur, R. S.; Potesilova, H.; Santavy, F. *Planta Med.* **1975**, *28*, 201−209.

(17) Bussotti, L.; Cacelli, I.; D'Auria, M.; Foggi, P.; Lesma, G.; Silvani, A.; Villani, V. *J. Phys. Chem. A.* **2003**, *107*, 9079−9085.

(18) Becke, A. D. *J. Chem. Phys.* **1993**, *98*, 5648−5652.

(19) Lee, C.; Yang, W.; Parr, R. G. *Phys. Rev. B: Condens. Matter Mater. Phys.* **1988**, *37*, 785.

(20) Tomasi, J.; Mennucci, B.; Cammi, R. *Chem. Rev.* **2005**, *105*, 2999.

(21) Frisch, M. J.; Trucks, G. W.; Schlegel, H. B.; Scuseria, G. E.; Robb, M. A.; Cheeseman, J. R.; Montgomery, J. A., Jr.; Vreven, T.; Kudin, K. N.; Burant, J. C.; Millam, J. M.; Iyengar, S. S.; Tomasi, J.; Barone, V.; Mennucci, B.; Cossi, M.; Scalmani, G.; Rega, N.; Petersson, G. A.; Nakatsuji, H.; Hada, M.; Ehara, M.; Toyota, K.; Fukuda, R.; Hasegawa, J.; Ishida, M.; Nakajima, T.; Honda, Y.; Kitao, O.; Nakai, H.; Klene, M.; Li, X.; Knox, J. E.; Hratchian, H. P.; Cross, J. B.; Bakken, V.; Adamo, C.; Jaramillo, J.; Gomperts, R.; Stratmann, R. E.; Yazyev, O.; Austin, A. J.; Cammi, R.; Pomelli, C.; Ochterski, J. W.; Ayala, P. Y.; Morokuma, K.; Voth, G. A.; Salvador, P.; Dannenberg, J. J.; Zakrzewski, V. G.; Dapprich, S.; Daniels, A. D.; Strain, M. C.; Farkas, O.; Malick, D. K.; Rabuck, A. D.; Raghavachari, K.; Foresman, J. B.; Ortiz, J. V.; Cui, Q.; Baboul, A. G.; Clifford, S.; Cioslowski, J.; Stefanov, B. B.; Liu, G.; Liashenko, A.; Piskorz, P.; Komaromi, I.; Martin, R. L.; Fox, D. J.; Keith, T.; Al-Laham, M. A.; Peng, C. Y.; Nanayakkara, A.; Challacombe, M.; Gill, P. M. W.; Johnson, B.; Chen, W.; Wong, M. W.; Gonzalez, C.; Pople, J. A. *Gaussian 03*, revision B.04; Gaussian, Inc.: Pittsburgh, PA, 2003.

(22) Cimiraglia, R. *J. Chem. Phys.* **1985**, *83*, 1746−1749.

(23) Huron, B.; Malrieu, J. P.; Rancurel, P. *J. Chem. Phys.* **1973**, *58*, 5745−5759.

(24) Werner, H.-J.; Knowles, P. J. *MOLPRO*, version 2002.1; University College Cardiff Consultants Limited: Cardiff, Wales, U. K., 2002.

(25) Bussotti, L.; D'Auria, M.; Foggi, P. G. L.; Righini, R.; Silvani, A. *Phothochem. Photobiol.* **2000**, *71*, 29−34.

(26) Calucci, L.; Cavazza, M.; Veracini, C. A.; Zandomeneghi, M. *J. Photochem. Photobiol., A* **1998**, *117*, 43.

(27) Joy, A.; Kammumalle, L. S.; Ramamurthy, V. *Org. Biomol. Chem.* **2005**, *3*, 3045.

(28) Croteau, R.; Leblanc, R. *Photochem. Photobiol.* **1978**, *28*, 33−38.

CT600306T